COUPLED SIMULATION ON FLUE GAS AND STEAM DEVIATION OF FINAL REHEATER IN A 600 MW TANGENTIALLY FIRED BOILER WITH REVERSED SEPARATED OVERFIRE AIR UNDER DIFFERENT LOADS

Zhengjiang WANG[1], Xingjun WANG[2], Yang YANG[1,3], Jiawei LI[2], Yongning SU[2], Qi JIANG[1], Xiaojun LI[1], Wenbin XING[2], Jinhao YI[3], Hu LIU[3,*]

[1] Xi'an TPRI Water-Management & Environmental Protection Co. Ltd., State Key Laboratory of High-Efficiency Flexible Coal Power Generation and Carbon Capture Utilization and Storage, Xi'an 710054, China

[2] Huaneng Longdong Energy Co., Ltd. Zhengning Power Plant, Qingyang 745306, China

[3] State Key Laboratory of Multiphase Flow in Power Engineering, School of Energy and Power Engineering, Xi'an Jiaotong University, Xi'an 710049, China

[*] Corresponding author; E-mail: epeliuhu@mail.xjtu.edu.cn

Flue gas and steam deviation of the final reheater is an inevitable problem in the tangentially fired boiler due to the remaining gas spinning at the furnace exit. An in-house one-dimensional process simulation code coupled with comprehensive three-dimensional combustion simulation was adopted to accurate investigate the characteristics of the flue gas and steam maldistribution of the final reheater in a 600 MW supercritical tangentially fired boiler. Firstly, the combustion simulation result was validated by the in-house fire-side heat transfer calculation data, then the effect of boiler loads and reversed separated overfire air (SOFA) deflection angles on the gas temperature deviation, velocity deviation and outlet steam temperature of reheater were conducted. The results showed that the deviation of flue gas temperature and velocity increases as the boiler load decreases. The reversed SOFA deflection angle plays a crucial role in improving the gas distribution under low loads, and the deviation of flue gas temperature and velocity is the smallest when the angle is -18° under 100% boiler maximum continuous rating (BMCR), 75% and 50% turbine heat acceptance (THA), but it is the smallest when the angle is -9° under 35% BMCR load. Moreover, the maximum outlet steam temperature difference between parallel heating surfaces of the final reheater increases from 84.68 K to 106.48 K as the boiler load decreases from 100% BMCR to 75% THA, and it is mainly affected by the flue gas temperature deviation rather than the mass flow rate maldistribution when the deflection angle changes from -9° to -18°.

Key words*: Coupled simulation; Temperature and velocity deviation; Steam temperature maldistribution; Reversed SOFA; Different loads*

1. Introduction

Renewable energy installation has been projected to grow rapidly in recent years due to the program of carbon emissions reduction in China, but the increased ratio of renewable energy generation caused several issues in the electrical power grid as its intermittent characteristics. Therefore, in order to ensure the stable and safe operation of power grid, most of the conventional coal fired power generation has to participate into deep peak regulating operation and the period of part loads operation significantly increased. Tangentially fired boilers have been widely used in the power generation industry since the advantage of a well-fulfilled flame in the furnace, high combustion efficiency, low NO_x emissions, and good coal adaptability [1-3]. However, the inherent gas spinning of tangential combustion system could cause gas temperature and velocity deviation in the furnace exit, which is proved to be the reason of local overheating and tube failure of the final reheater and the final superheater [4, 5], especially when the boiler operate at part loads [6].

The issue of flue gas deviation and the measure to mitigate it have received widespread attention, but the on-site test is difficult to provide complete data due to the size and the complexity of the equipment [7]. Therefore, numerical methods have been widely adopted to provide guidance for the practical process in recent years [8-12]. Xu et al. [13] numerical studied and found that the remaining gas spinning was responsible for the gas temperature deviation, as the different residence time and temperature of spinning upward flue gas on both sides in the platen zone resulted in uneven heat transfer. Yin et al. [14] studied the gas temperature deviation in a 609 MW boiler and concluded that the platen superheater could mitigate rather than strengthen the deviation, since it could improve the uniformity of the flue gas velocity. Yang et al. [15] believed that nonlinearity high Reynolds number flow was prone to generate asymmetrical distribution of velocity and temperature under BMCR condition.

Some measures have been carried out to mitigate the negative effects of the flue gas deviation on the operation economy and safety in the tangentially fired boiler. He et al. [16] reported that tilting downward the overfire air jet can reduce the remaining gas spinning and improve the mixing process between the primary and secondary air flows. Zhou et al. [17] conducted a numerical and experimental study, and found that opposing tangential primary air jets were able to reduce the imaginary circle diameter and the spinning momentum intensity at the furnace exit in the large-scale tangentially fired boiler. Moreover, they reported that there was an appropriate range of opposing tangential angles, and the reasonable changes of the furnace arch structure and division platen superheaters arrangements could also play a role. Yan et al. [18] found that wall tangentially fired system can generate a more uniform and symmetric velocity distribution in the upper furnace, and reduce the flue gas temperature deviation at the furnace exit. Chen et al. [19] reported that the arrangement of wall center tangentially fired system shows the best uniform distribution of velocity, temperature, species concentration, and heat fluxes of the furnace water-cooled wall. Li et al. [20] innovative proposed an annularly combined multiple airflows scheme, and compared with the conventional wall tangentially fired system, the flue gas deviation and furnace fullness were obviously improved.

Air staging technology which is typically adopted as an effective way to reduce NO_x emissions [21, 22] can also mitigate the spinning intensity at furnace exit [5, 23-25]. Tian et al. [26] found that tilting upward the main burners and SOFA nozzles are both useful to reduce the spinning intensity in a 700 MW boiler, and the on-site experiment indicated that the combination of burner tilt angle of 11° and the SOFA tilt angle 10° can obtain an optimum mitigation of steam temperature deviation. Liu et

al. [25] reported that the deeper the air staging, the more intense of the remaining gas spinning, and the greater thermal deviation of the final superheater. Ping et al. [5] found that the air staging technology could cause the burnout delay of pulverized coal particles, and the maldistribution of pulverized coal particles is responsible for the thermal deviation of the final reheaters [27].

All the above-mentioned studies only focus on the temperature and velocity deviation of flue gas, include the arrangement of burners, title angle of burner and air staging condition. In fact, the local overheating is not only caused by the flue gas deviation, but also the unevenly distribution of working fluid among the tubes of the heating surface [3], and the method combined the flue gas side and fluid side can obtain more accurate analysis of thermal deviation. Some scholars [28] have already combined 3-D combustion simulation on the flue gas side with 1-D process simulation on the fluid side to analyze the thermal deviation. Bhargav et al. [29] adopted a 1-D and 3-D hybrid model to simulate the convective heat transfer in the boiler tube. Yu et al. [30] coupled the 3-D combustion model and 1-D thermal hydraulic model to consider the heat transfer on the flue gas and fluid sides, they found that 0.16% of the outer surface of the final reheater exceed the limitation metal temperature when the SOFA tilt angle increases from + 20° to + 30°. Norbert et al. [31] proposed numerical procedure to couple the 3-D flue gas side simulation with 1-D pipe flow model in the heat exchanger, and the numerical method was used to optimize the reheater design to achieve uniform tube metal temperature. In our previous work, the combustion simulation and the in-house hydrodynamics model were combined to investigate the steam temperature and metal temperature of water-cooled wall [32-34], and the results of combined model agree well with the in-situ data. These studies have proven combined method to be a feasible and powerful tool for analyzing the thermal deviation in tangentially fired boiler.

However, most of the previous studies only conducted the temperature and velocity deviation of fire side, and the deflection angle of reversed SOFA on thermal deviation under different loads especially part loads were also lack of enough attention and research. Therefore, the 3-D combustion simulation coupled with in-house 1-D process simulation was adopted to accurate analyze the effect of reversed SOFA deflection angle on the outlet steam temperature and mass flow rate of the final reheater in a 600 MW full-scale tangentially fired boiler in this study.

2. Computational methodology

2.1. The tangentially fired boiler and cases set up

A 600 MW supercritical tangentially fired boiler with a single furnace and deep air-staging combustion system is studied. The structure of the boiler is displayed in Figure 1. The height of the furnace is 63.75 m, with 18.816 m in width and 17.696 m in depth. Six levels of LNCFS burners with two layers of CCOFA nozzles and five layers of SOFA nozzles located at each corner to reduce NO_x emissions, one layer of UFA nozzles is arranged at the bottom of the burner. Furthermore, the nozzles of CFS is deviated 20° clockwise from the PA nozzles to form a strong oxidizing atmosphere and protect the water-cooled wall from high-temperature corrosion, as shown in Figure 1 (b). The yaw angle of the reversed SOFA nozzles can be horizontally changed, but the UFA, SA, and CCOFA are fixed.

The calculation domains are shown in Figure 1 (c). The horizontal planes P1 (Y = 25.46 m) and P2 (Y = 32.87 m) denotes the cross-sections of burners A and E, respectively. P3 (Y = 40.00 m) is

located in a horizontal plane with a height of 40 m and P4 (Y = 44.10 m) is located in the cross-section of SOFA-C. The exit of the furnace nose is marked as P5 (Y = 56.35 m). In the crossover pass, the vertical cross-sections Q1 (X = 10.24 m) and Q2 (X = 12.46 m) are located in the entrance and exit of the platen superheater. In the horizontal pass, Q3 (X = 15.94 m) represents the exit of the final reheater, and Q4 (X = 18.69 m), Q5 (X = 23.13 m) is respectively the entrance and exit of the final superheater.

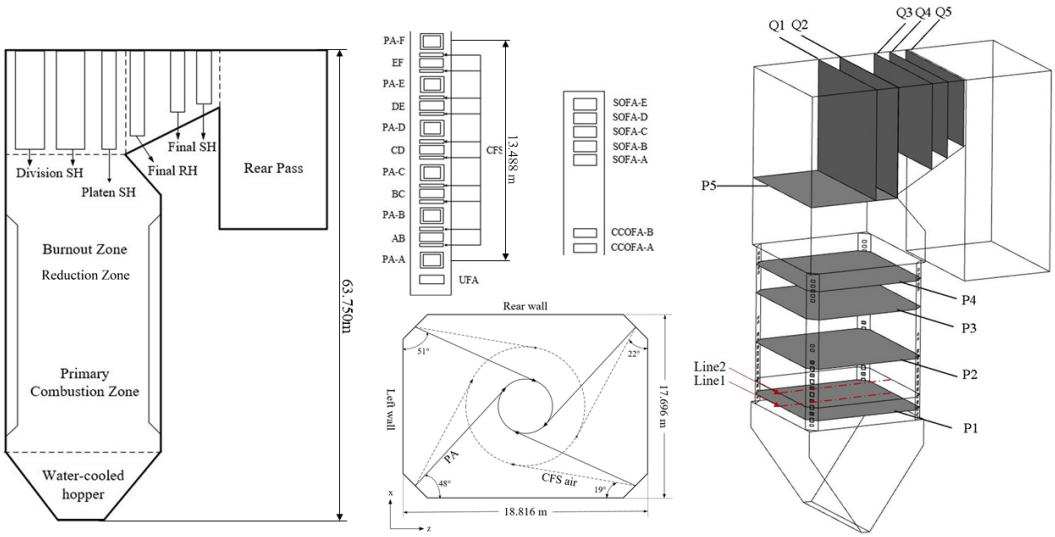

(a) Boiler configuration (b) Burners arrangement and yaw angles (c) Calculating planes

Figure 1. Schematic diagram of boiler

In the present study, the influence of reversed tangential angle of SOFA on gas temperature, velocity and steam deviation were researched under different loads. The main parameters under different SOFA deflection angle and boiler loads are listed in Table 1, and different layers of pulverized coal nozzles were on service. Case 1 to case 4 are set to explore the influence of different loads on the maldistribution phenomenon, in which the yaw angle of SOFA nozzles is fixed at 0°. Case 5 to case 12 are set with two SOFA deflection angles (-9°, -18°). Table 2 presents the proximate and ultimate analysis of the coal fed to the boiler.

Table 1. Operation parameters for all the cases

Cases	Load	Coal feed rate (t/h)	Reversed tangential angle of SOFA, α	Excess air coefficient	Secondary air temperature (K)
case 1	100% BMCR	240.0	0°	1.20	612
case 2	75% THA	164.4	0°	1.33	579
case 3	50% THA	113.0	0°	1.37	551
case 4	35% BMCR	95.7	0°	1.47	540
case 5	100% BMCR	240.0	-9°	1.20	612
case 6	100% BMCR	240.0	-18°	1.20	612
case 7	75% THA	164.4	-9°	1.33	579
case 8	75% THA	164.4	-18°	1.33	579
case 9	50% THA	113.0	-9°	1.37	551
case 10	50% THA	113.0	-18°	1.37	551
case 11	35% BMCR	95.7	-9°	1.47	540

case 12	35% BMCR	95.7	-18°	1.47	540

Table 2. The proximate and ultimate analyses of coal sample

Proximate analysis (wt%, as received)				Ultimate analysis (wt%, as received)					LHVar (MJ/kg)
FC	A	V	M	C	H	O	N	S	
47.56	11.26	26.18	15.00	59.41	3.48	9.47	0.80	0.58	22.66

2.2. Calculation and evaluation method

A commercial CFD software ANSYS FLUENT was used to carry out the 3-D simulation of coal combustion. SIMPLE algorithm was chosen to solve the time average conservation equations for energy, mass, and momentum. The diameter distribution of the pulverized coal followed Rosin-Rammler function with a mean diameter of 61 μm, a minimum diameter of 1 μm, and a maximum diameter of 200 μm. Realizable *k-ε* model which is supposed to perform better in the swirling flow is adopted to consider the high turbulence intensity characteristic of the gas flow pattern in the boiler [19, 35]. The near-wall treatment was considered by standard wall functions. The process of coal devolatilization was modeled using two-competing-reaction model, and the radiation heat transfer process was calculated by the discrete ordinates model. Besides, finite-rate/eddy-dissipation was used to model the turbulence-chemistry interaction of gas phase. And the kinetic/diffusion surface reaction model was used to model the char particles combustion [36]. Weighted-sum-of-gray-gases model was adopted to calculate absorption coefficients of the gas phase [28, 37].

The velocity and temperature distribution of flue gas are affected by multiple factors such as primary air rate, secondary air rate, nose structure and nozzles arrangement. In order to quantitatively describe the swirl strength, the spinning momentum intensity is introduced, which is represented by ψ, and the definition of ψ is as follows [25]:

$$\psi = 2\pi \int_0^R \rho\omega^2 r^2 \mathrm{d}r = \oiint \rho\omega^2 r \mathrm{d}A \tag{1}$$

In addition, E_T and E_V are introduced to give a quantitative description of the temperature and velocity deviation of the flue gas [26, 38]:

$$E_T = \frac{T_{\mathrm{ave,l}}}{T_{\mathrm{ave,r}}}, E_V = \frac{V_{\mathrm{ave,l}}}{V_{\mathrm{ave,r}}} \tag{2}$$

As the ratio of two values, the closer E_T and E_V are to 1, the closer the temperature and velocity of the two half planes are.

The final reheater installed in the boiler is composed of parallel U-tubes and the steam flow inside is superheated steam. The pressure drops due to gravity and acceleration of reheat steam flow are both negligible in U-tube. Consequently, the single-phase pressure drop in a single tube can be described as follows [39],

$$\Delta p = \Delta p_f + \Delta p_j \tag{3}$$

$$\Delta p_f = \lambda \frac{l}{d_{in}} \frac{G^2}{2} \nu \tag{4}$$

$$\Delta p_j = \xi \frac{G^2}{2} \nu \tag{5}$$

The detailed description of the 1-D process model can be found in our previous work [32-34].

On the basis of the thermal load, pressure drop, and the flow rate, the steam temperature could be obtained by enthalpy. The relation between *T*, *P*, and *h* are as follows,

$$T = f\left(P, h\right) \tag{6}$$

The coupled method is that, firstly, the amount of heat absorption on the heating surface and the outlet temperature of the heating surface both were determined with the thermal performance calculation software proposed by the present group and proved by many actual projects. Next, the numerical simulation of combustion in the furnace was conducted with CFD software, and the thermal performance calculation data was adopted to verify the numerical model, then, the numerical models were used to simulate the combustion to determine the heat flux distribution of the heating surface under different loads. Subsequently, the hydrodynamic calculation model was established and the heat flux distribution of the heating surface was adopted to calculate the steam temperature of the heating surface. Finally, the results were used to analyze the deviation characteristics of the heating surface.

2.3. Grid independent test

A grid independence test was carried out on case 1 with four mesh systems of 1 337 476, 1 752 193, 2 067 250, and 2 478 099 hexahedral cells. Figure 2 shows the temperature and velocity of different grid numbers on the centerlines along the depth Line 1 (Y = 25.459 m, Z = -9.408 m, X = 0 to 17.696 m) in the PA-A cross-section and Line 2 (Y = 27.307 m, Z = -9.408 m, X = 0 to 17.696 m) in the PA-B cross-section. It is obvious that the computational results of 2 067 250 and 2 478 099 hexahedral cells are extremely close. Therefore, the mesh system of 2 067 250 was selected in the present work.

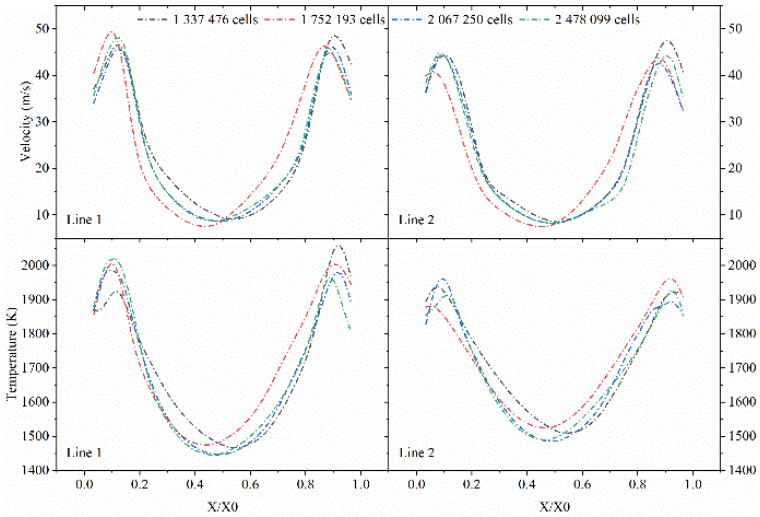

Figure 2. The simulation results of four mesh systems

3. Results and discussion

3.1. Validation of numerical simulation

The simulated flue gas temperature was compared with the in-house heat transfer calculation model of fire side [34] to validate the simulation models [40-42], and the temperature comparison of several cross-sections including Q1-Q5 for case 1 is indicated in Figure 3. It can be seen that the simulation data show a good agreement with the in-house model value, and the relative errors are within 8% on the whole. The deviation could be partly attributed to the intrinsic distinction between

the methods of sampling since one is the zero-dimensional calculation value and the other is the area-weighted average temperature. Therefore, the numerical model is reliable to predict the characteristics of the combustion, flow, and heat transfer in the boiler.

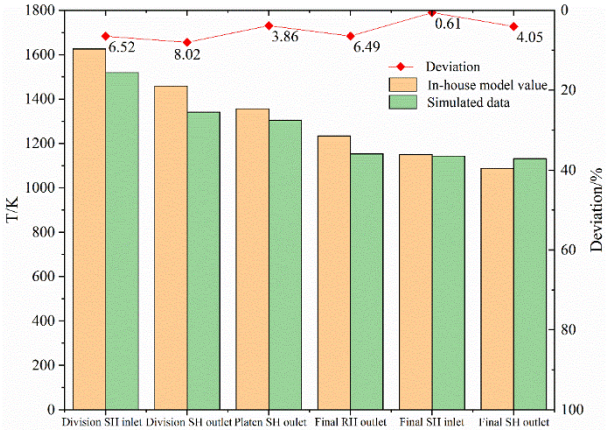

Figure 3. Comparison of the in-house model calculated and simulated temperature for case 1

3.2. The flue gas velocity and temperature distribution at the inlet of final reheater

Figure 4 shows the temperature and velocity distributions of the longitudinal section at the center of the furnace and the planes P1, P2, P4, and Q2 for case 1, which is the basic condition with the reversed tangential SOFA at 0^{o} under 100% BMCR load. It can be seen that the temperature and velocity distribution are similar, and the tangentially imaginary circle is formed, which is attributed to the arrangement of the nozzles of the tangentially fired system. In the primary combustion zone, the air and pulverized coal mixture are injected into the furnace and heated by the neighboring upstream high temperature flue gas, then the pulverized coal experience devolatilization, ignition and combustion. Therefore, the clockwise tangential circle is formed by the jets from four corners at the furnace center. Moreover, in the burnout zone, SOFA is injected into the furnace with great momentum, which strengthen the spinning momentum intensity. As a result, the remaining gas spinning is observable when the flue gas reach furnace exit.

Although the platens can weaken the remaining gas spinning flow to some extent, the non-uniformity of gas temperature and velocity caused by swirl flow is still considerable in the horizontal flue pass where the final reheater is installed. Figure 5 shows the distributions of flue gas velocity and temperature of the flue gas inlet of the final reheater (Q2 plane). The dimensionless number *Y/Y0* and *Z/Z0* is defined to illustrate the change of location along height and width of horizontal pass, respectively. In details, the relative height *Y/Y0* is defined as the ratio of the height of the point to the horizontal pass height, and the relative width *Z/Z0* represents the location of the point along the horizontal direction. As it can be seen, flue gas velocity tends to be uniform as the increase of *Y/Y0*, and the gas temperature shows the same trend. The flue gas velocity on the left side is obviously higher than that on the right side as *Y/Y0* increases from 0.2 to 0.68, especially in the lower area, but the velocity on the right side exceeds the value of the left side when *Y/Y0* is equal to 0.84. In addition, the lowest temperature and velocity both appear in the right bottom area.

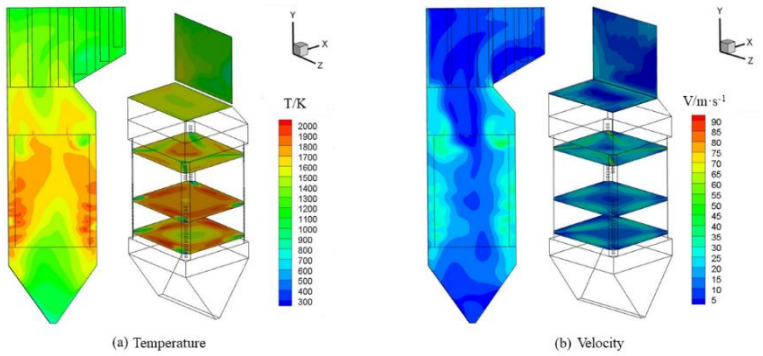

Figure 4. Distribution of temperature and velocity in the furnace

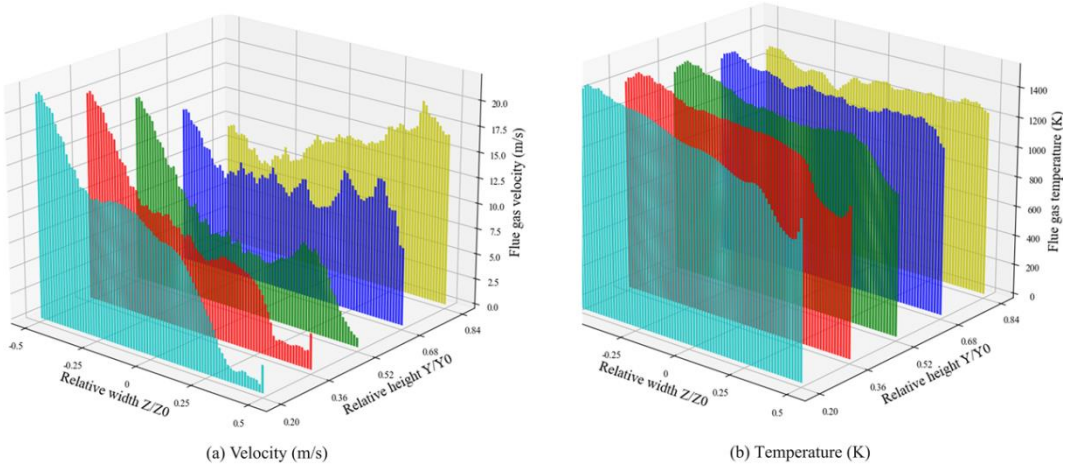

Figure 5. Distribution of flue gas velocity and temperature in Q2 along *Y/Y0* and *Z/Z0*

3.3. The temperature and velocity deviation under different loads

Figure 6 shows temperature distribution and streamlines in vertical planes about 0.5 m away from the left and right wall at the upper furnace under different loads. It can be seen that there is significant difference between the left and right planes under all the four loads, and the low-temperature area appears at the lower right corner of the horizontal pass. The reason is that, the clockwise swirling flue gas changes its direction to the horizontal pass when it flows out of the furnace, the flue gas near the left side directly flows to the horizontal pass under the guidance of division superheater and platen superheater. The flue gas temperature maintains high, the path distance and residence time of this part flue gas is short, thus the heat exchange with the division superheater and platen superheater is insufficient. But the flue gas near the right side tends to flow to the front wall first, then change its direction to upward as the restriction of front wall, finally, the flue gas flow backward to the horizontal pass as the restriction of furnace roof. Therefore, the gas trajectory near the right side presents “C” shape. Moreover, there is a recirculation zone generates near the junction of the front wall and the furnace roof and the lower right area of the horizontal flue pass, respectively. Besides, the flue gas velocity and temperature are relatively low in this area, and the recirculation zone expands with the decrease of boiler load, since the mass flow rate decreases and consequently the furnace fullness decreases as the decrease of the boiler load.

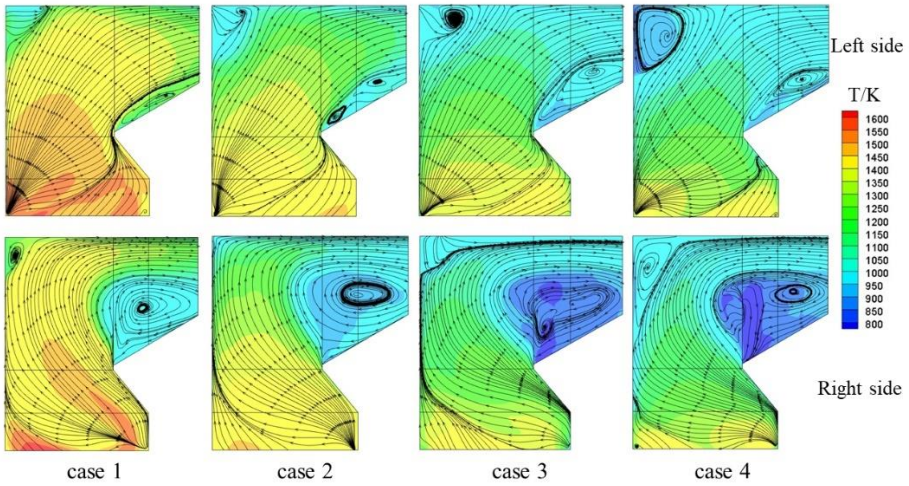

Figure 6. Temperature distribution and streamlines in vertical cross-sections next to the left wall and right wall in the upper furnace

Figure 7 shows the distribution of spinning momentum intensity ψ along the height of the furnace for case 1 to case 4. Dimensionless height *H/H0* indicates the altitude ratio of the calculating plane to the boiler total height. As can be seen from Figure 7, ψ shows similar trends for case 1 to case 4. For all the cases, ψ is high in the primary combustion zone and burnout zone, especially the layers of burner nozzles and SOFA nozzles since the air injected into the furnace from these nozzles. But ψ falls off and maintains at a relatively low level in the reduction zone owing to no addition of PA or SA, and the spinning value decreases sharply after the SOFA injected into the furnace. Moreover, ψ is 22 196 N • m, 13 596 N • m, 6 611 N • m, 3 068 N • m for case 1 to case 4 at the furnace exit, which means the fewer the burners are on service, the lower the remaining gas spinning momentum intensity.

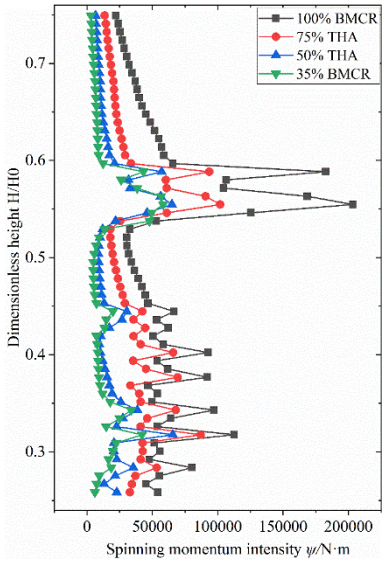

Figure 7. Distribution of calculating spinning momentum intensity along *H/H0* for cases 1 to 4

Figure 8 shows the distribution of E_T and E_V in Q2 plane under different loads. As it can be seen, E_T and E_V are larger than 1 under all the cases due to the clockwise gas flow spinning. In detail, E_T rises from 1.082 to 1.151, and E_V rises from 1.212 to 1.622, as the boiler load decreases from 100%

to 35% BMCR. To summarize, temperature and velocity deviation coefficient increase as the decrease of the load, which means the deviation degree becomes more serious when the boiler under part load.

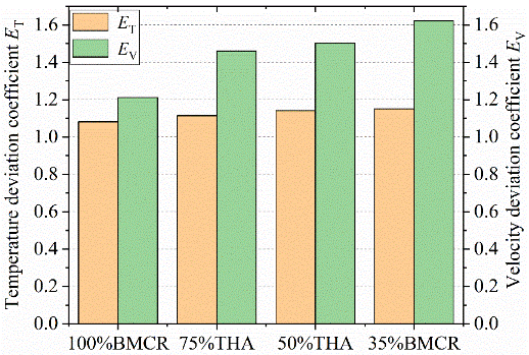

Figure 8. E_T and E_V in plane Q2 for case 1 to case 4 under different loads

3.4. The influence of reversed SOFA

3.4.1 The characteristics of the flue gas distribution

Reversed SOFA is superior to reversed primary air and auxiliary air since the former has little effect on the flow field and the ignition of pulverized coal in the furnace. Therefore, the SOFA nozzles, which are arranged close to each other, can be adopted to weaken the gas spinning momentum intensity. Figure 9 illustrates the spinning momentum intensity of all the cases. It can be seen that the spinning momentum intensity of the furnace exit decreases as the deflection angle of SOFA decreased, and it has little effect on the primary combustion zone. Moreover, there is no significant difference at the furnace exit when the deflection angle α changes from -9° to -18° under 35% BMCR, which means that the method of reversed tangential SOFA may not work under extremely low load, although it has a strong effect on the attenuation of the gas spinning intensity under full load.

Figure 10 shows the streamlines in horizontal plane P4 and P5 under 100% and 35% BMCR load. As can be seen in Figure 10 (a), the diameter of the tangential circle in the center formed by clockwise spinning flue gas gradually decreases as the increase of α. The reason is that the reversed SOFA slowed down the velocity of flue gas flow. In other words, the non-uniform distributed flue gas at the furnace exit could be alleviated by setting a deflection angle of SOFA. However, changing the reversed SOFA deflection angles is not work at the low load. Figure 10 (b) and Figure 10 (c) show the streamlines in P4 and P5, which reveals the gas flow condition in the burnout zone and the furnace exit under 35% BMCR, respectively. It can be seen that the original flue gas distribution in the burnout zone under low load forms a tangential circle with a small diameter, but when the deflection angle of SOFA is -18°, the flue gas changes its spinning direction and the reversed spinning momentum intensity is even strengthened in P5, since the spinning momentum intensity is weak and the spinning direction is relatively easy to be changed by the injection of SOFA under 35% BMCR load. Therefore, it can be inferred that if α exceeds -18°, the gas spinning momentum intensity will be more intense, which means there is a proper range of reversed tangential angle of SOFA to mitigate the remaining gas spinning, particularly under low loads, and the most appropriate value of α should be in the range of -9° to -18° under 35% BMCR in this study.

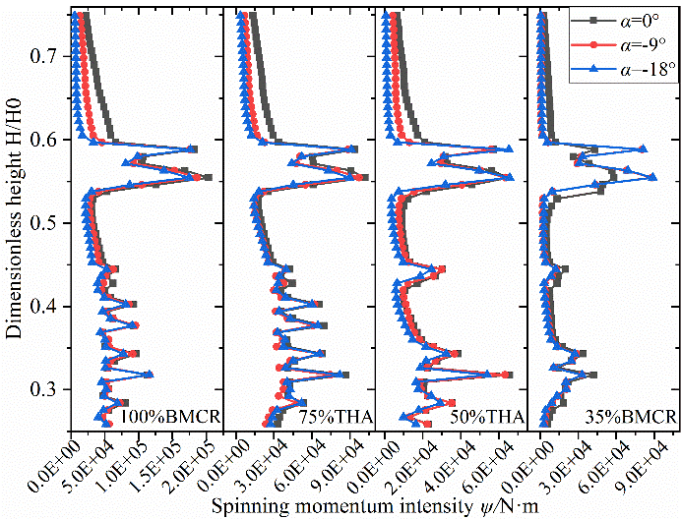

Figure 9. Distribution of calculating spinning momentum intensity along *H/H0* at different loads and different deflection angle

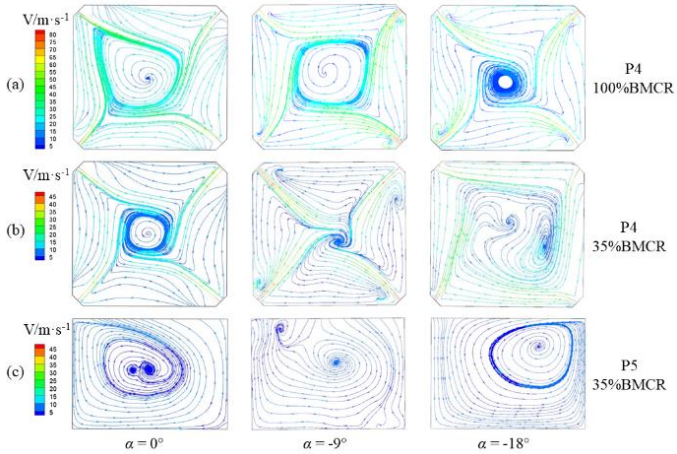

Figure 10. Streamlines at different loads and different *α*

Figure 11 shows the results of E_T and E_V of the vertical plane Q2 for all the conditions. It can be seen that E_T and E_V decrease with the increase of α, and the decrease rate increase with the decrease of the boiler load. For instance, when α changes from 0° to -18°, E_T reduces by 0.08 under 100% BMCR while by 0.312 under 35% BMCR, which demonstrates that the reversed SOFA plays a more crucial role under low loads. Whereas, it should be emphasized that E_V and E_T are far below 1 in case 12, which means the spinning momentum intensity of the gas is strengthened by the reversed trend. Hence, the remaining gas spinning reveals a reversed trend at a low load, since the gas temperature and velocity on the left are significantly lower than those on the right in the entrance of the final reheater.

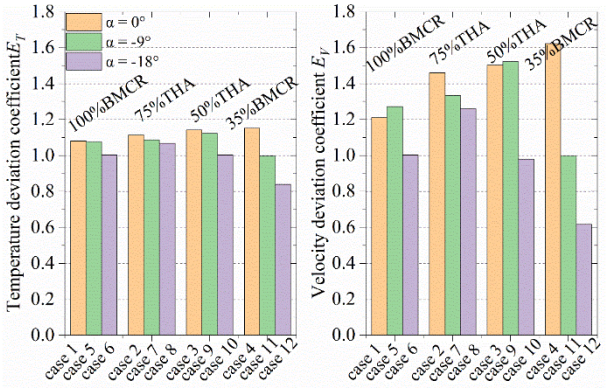

Figure 11. Deviation coefficient of Q2 for all the cases

3.4.2 The appearance of the reheat steam

As an effective method to mitigate the nonuniformity of the gas temperature and gas velocity, reversed tangential SOFA can improve the distribution of steam flow rate and outlet temperature. Figure 12 illustrate the maximum differences in steam temperature and flow rate, and both of them significant decrease as α changes from 0° to -18° in almost all of the cases, except for case 12 which operates at 35% BMCR. In case 12, the high-temperature flue gas leans to the right side rather than the left side which is different from the other 11 cases. What is more, the mass flow rate of reheat steam decreases with the decrease of the boiler load, which aggravates the outlet steam temperature difference. The maximum steam temperature difference appeared under case 12 proves that the optimize range of α under 35% BMCR is between -9° and -18°. Moreover, it is apparent that the flow rate difference significantly decreased when α change from -9° to -18°, which represents that the deflection angle of SOFA with a moderate value is sufficient to improve the steam flow distribution, and it can be concluded that the flue gas temperature deviation rather than the mass flow rate distribution of the steam is the main reason for the steam temperature difference when α varies from -9° to -18°.

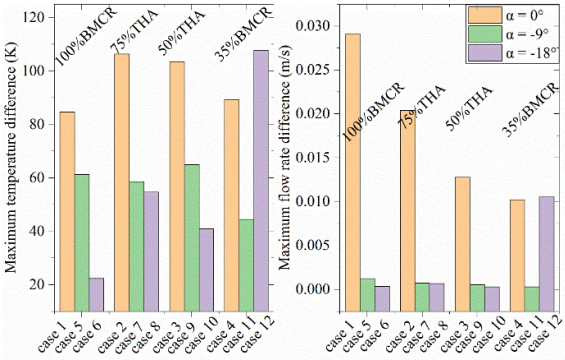

Figure 12. Maximum temperature and flow rate differences of the reheat steam for all the cases

4. Conclusions

In this study, a validated coupled numerical simulation model was adopted to investigate the impact of reversed SOFA deflection angle on flue gas and steam deviation under different loads in a 600 MW supercritical tangentially fired boiler with a deep air-staging combustion system. The impact of boiler load and reversed SOFA deflection angle on the gas temperature and velocity deviation at the

inlet cross-section of the final reheater was discussed, then the steam temperature difference and steam flow rate difference of the final reheater was studied. Based on the simulation results, the following conclusions could be drawn.

The spinning momentum intensity decreases as the decrease of the boiler load. On the contrary, E_T rises from 1.082 to 1.151, and E_V rises from 1.212 to 1.622 when the boiler load changes from 100% BMCR to 35% BMCR.

The reversed SOFA is effective in mitigating the maldistribution of the gas temperature and gas velocity under most loads, but it may not work when the deflection angle is big enough under low loads, since E_T and E_V are far below 1 when the deflection angle is -18° under 35% BMCR. The most appropriate value of α should be in the range of -9° to -18° under 35% BMCR load.

The steam outlet temperature difference is mainly affected by the flue gas deviation, since the maximum difference of the outlet temperature increases from 84.68 K to 106.48 K as the boiler load decreases from 100% BMCR to 75% THA, but the flow rate difference falls much less when α changes from -9° to -18°.

Acknowledgment

This work was financially supported by the Science and Technology Project of China Huaneng Group Co., Ltd. (HNKJ21-H44).

Nomenclature

Acronyms

BMCR	boiler maximum continuous rating	CCOFA	close-coupled overfire air
CFD	computational fluid dynamics	CFS	concentric firing system
D	dimensional	LNCFS	low-NO_x concentric firing system
PA	primary air	SA	secondary air
SOFA	separated overfire air	THA	turbine heat acceptance
UFA	under-fire air		

Variables

d	diameter [m]	E	deviation coefficient [-]
G	mass velocity [$kg\cdot(m^2\cdot s)^{-1}$]	h	enthalpy [$kJ\cdot kg^{-1}$]
l	tube length [m]	P	pressure [MPa]
r	rotating radius [m]	R	equivalent radius [m]
T	fluid temperature [K]	V	gas velocity[$m\cdot s^{-1}$]

Greek symbols

Δ	loss	λ	heat conductivity coefficient [$W\cdot(m\cdot K)^{-1}$]
ν	specific volume of medium [$m^3\cdot kg^{-1}$]	ξ	local resistance coefficient [-]
ρ	flue gas density [$kg\cdot m^{-3}$]	ψ	spinning momentum intensity [N·m]
ω	tangential velocity [$m\cdot s^{-1}$]		

Subscripts

ave	area-weighted average	f	friction resistance
in	tube inner	j	local resistance
l	left half of the plane	r	right half of the plane

T temperature V velocity

References

[1] Yao, Z., *et. al.*, Numerical investigation of 700 °C boiler flue gas thermal deviation based on orthogonal experiment, *Fuel, 295* (2021), 120510

[2] Liu, H., *et. al.*, Effect of FGR position on the characteristics of combustion, emission and flue gas temperature deviation in a 1000 MW tower-type double-reheat boiler with deep-air-staging, *Fuel, 246* (2019), pp. 285-294

[3] Che, D.F., *Boilers-Theory, Design and Operation*, Xi'an Jiaotong University Press, Xi'an, China, 2008

[4] Wu, X., *et. al.*, Numerical simulation research on the unique thermal deviation in a 1000 MW tower type boiler, *Energy, 173* (2019), pp. 1006-1020

[5] Ping, L., *et. al.*, Measurement of thermal deviation of flue-gas in crossover pass of single tangential boiler, *Appl. Therm. Eng.*, *188* (2021), 116647

[6] Laubscher, R., Rousseau P., CFD study of pulverized coal-fired boiler evaporator and radiant superheaters at varying loads, *Appl. Therm. Eng.*, *160* (2019), 114057

[7] Díez, L.I., *et. al.*, Numerical investigation of NO_x emissions from a tangentially-fired utility boiler under conventional and overfire air operation, *Fuel, 87* (2008), 7, pp. 1259-1269

[8] Belosevic, S., *et. al.*, A numerical study of a utility boiler tangentially-fired furnace under different operating conditions, *Fuel, 87* (2008), 15, pp. 3331-3338

[9] Kuang, M., *et. al.*, In-furnace flow field, coal combustion and NO_x emission characteristics regarding the staged-air location in a cascade-arch down-fired furnace, *J. Energy Inst.*, *98* (2021), pp. 259-270

[10] Wang G., *et. al.*, Numerical simulation of pulverized coal combustion in a rotary kiln under O_2/CO_2 atmosphere, *Therm. Sci.*, *27* (2023), 6B, pp. 4935-4945

[11] Crnomarković, N. Dj., *et. al.*, Influence of the temperature fluctuations on the flame temperature and radiative heat exchange inside a pulverized coal-fired furnace, *Therm. Sci., 27* (2023), 6A, pp. 4539-4549

[12] Dostiyarov, A., *et. al.*, Experimental and numerical study of the double stage burner with vortex generator, *Therm. Sci.*, 2024, Online first, https://doi.org/10.2298/TSCI220318140D

[13] Xu, M., *et. al.*, Simulation of the gas temperature deviation in large-scale tangential coal fired utility boilers, *Comput. Method. Appl. M.*, *155* (1998), 3, pp. 369-380

[14] Yin, C., *et. al.*, Further study of the gas temperature deviation in large-scale tangentially coal-fired boilers, *Fuel, 82* (2003), 9, pp. 1127-1137

[15] Yang, M., *et. al.*, Numerical investigation of the nonlinear flow characteristics in an ultra-supercritical utility boiler furnace, *Appl. Therm. Eng.*, *88* (2015), pp. 237-247

[16] He, B., *et. al.*, Computational fluid dynamics based retrofits to reheater panel overheating of No. 3 boiler of Dagang Power Plant, *Comput. Fluids, 36* (2007), 2, pp. 435-444

[17] Zhou, Y., *et. al.*, Effect of opposing tangential primary air jets on the flue gas velocity deviation for large-scale tangentially fired boilers, *Energ. Fuel., 23* (2009), 11, pp. 5375-5382

[18] Yan, L., *et. al.*, Numerical simulation of a 600 MW utility boiler with different tangential arrangements of burners, *Energ. Fuel., 26* (2012), 9, pp. 5491-5502

[19] Chen, S., *et. al.*, Numerical investigations on different tangential arrangements of burners for a 600 MW utility boiler, *Energy, 122* (2017), pp. 287-300

[20] Li, Z., *et. al.*, A novel burner arrangement scheme with annularly combined multiple airflows for wall-tangentially fired pulverized coal boiler, *Energy,* 222 **(**2021), 119912

[21] Choi, C. R., Kim C. N., Numerical investigation on the flow, combustion and NO_x emission characteristics in a 500 MWe tangentially fired pulverized-coal boiler, *Fuel, 88* (2009), 9, pp. 1720-1731

[22] Zhou, H., *et. al.*, Modeling and optimization of the NO_x emission characteristics of a tangentially fired boiler with artificial neural networks, *Energy, 29* (2004), 1, pp. 167-183

[23] Wu, X., *et. al.*, Numerical simulation research on the unique thermal deviation in a 1000 MW tower type boiler, *Energy, 173* (2019), pp. 1006-1020

[24] Ribeirete, A., Costa M., Detailed measurements in a pulverized-coal-fired large-scale laboratory furnace with air staging, *Fuel, 88* (2009), 1, pp. 40-45

[25] Liu, Y. C., *et. al.*, Experimental and numerical studies on the gas velocity deviation in a 600 MWe tangentially fired boiler, *Appl. Therm. Eng., 110* (2017), pp. 553-563

[26] Tian, D., *et. al.*, Influence of vertical burner tilt angle on the gas temperature deviation in a 700 MW low NO_x tangentially fired pulverised-coal boiler, *Fuel Process. Technol., 138* (2015), pp. 616-628

[27] Xie, J., *et. al.*, Thermal deviation analysis of high-temperature reheater for single-tangential π type boiler, *Appl. Therm. Eng., 192* (2021), 116846

[28] Chen, T., *et. al.*, Coupled modeling of combustion and hydrodynamics for a coal-fired supercritical boiler, *Fuel, 240* (2019), pp. 49-56

[29] Akkinepally, B., *et. al.*, Numerical and experimental study on biased tube temperature problem in tangential firing boiler, *Appl. Therm. Eng., 126* (2017), pp. 92-99

[30] Yu, C., *et. al.*, Numerical investigation of combustion optimization in a tangential firing boiler considering steam tube overheating, *Appl. Therm. Eng., 154* (2019), pp. 87-101

[31] Modliński, N., *et. al.*, Mathematical procedure for predicting tube metal temperature in the second stage reheater of the operating flexibly steam boiler, *Appl. Therm. Eng., 146* (2019), pp. 854-865

[32] Yuan, M., *et. al.*, Coordinate transformation method for heat reallocation in the spiral water-cooled wall temperature calculation, *Int. J. Therm. Sci., 177* (2022), 107557

[33] Liu, H., *et. al.*, Coupled modeling of combustion and hydrodynamics for a 1000 MW double-reheat tower-type boiler, *Fuel, 255* (2019), 115722

[34] Liu, H., *et. al.*, Coupled combustion and hydrodynamics simulation of a 1000 MW double-reheat boiler with different FGR positions, *Fuel, 261* (2020), 116427

[35] Kim, K. M., *et. al.*, Development of Subair Technique for Combustibility Enhancement and NO_x Reduction in a Pulverized Coal-Fired Boiler, *ACS Omega*, *4* (2019), 1, pp. 2291-2301

[36] Jiang, Y., *et. al.*, Optimization of separated overfire air to reduce NO_x emissions under combustion stability for the retrofit of a 500 MW tangentially pulverized coal boiler, *Fuel, 289* (2021), 119764

[37] Liu, Y., *et. al.*, Numerical investigation of air-staged combustion emphasizing char gasification and gas temperature deviation in a large-scale, tangentially fired pulverized-coal boiler, *Appl. Energy, 177* (2016), pp. 323-334

[38] Tan, P., *et. al.*, Causes and mitigation of gas temperature deviation in tangentially fired tower-type boilers, *Appl. Therm. Eng., 139* (2018), pp. 135-143

[39] Hu, Y. P., *Power plant boiler handbook*, China Electric Power Press., Beijing, 2005 (in Chinese)

[40] Yin, C., *et. al.*, Investigation of the flow, combustion, heat-transfer and emissions from a 609 MW utility tangentially fired pulverized-coal boiler, *Fuel, 81* (2002), 8, pp. 997-1006

[41] Guo, J., *et. al.*, Numerical investigation on oxy-combustion characteristics of a 200 MWe tangentially fired boiler, *Fuel, 140* (2015), 2, pp. 660-668

[42] Edge, P. J., *et. al.*, An integrated computational fluid dynamics–process model of natural circulation steam generation in a coal-fired power plant, *Comput. Chem. Eng., 35* (2011), 12, pp. 2618-2631

Received: 17.05.2024.
Revised: 25.07.2024.
Accepted: 01.08.2024.